AIP ADVANCES **3**, 082105 (2013)

# Giant secondary grain growth in Cu films on sapphire[a]

David L. Miller,[b] Mark W. Keller,[c] Justin M. Shaw, Katherine P. Rice, Robert R. Keller, and Kyle M. Diederichsen
*National Institute of Standards and Technology, Boulder, CO 80305, USA*

(Received 14 June 2013; accepted 23 July 2013; published online 2 August 2013)

Single crystal metal films on insulating substrates are attractive for microelectronics and other applications, but they are difficult to achieve on macroscopic length scales. The conventional approach to obtaining such films is epitaxial growth at high temperature using slow deposition in ultrahigh vacuum conditions. Here we describe a different approach that is both simpler to implement and produces superior results: sputter deposition at modest temperatures followed by annealing to induce secondary grain growth. We show that polycrystalline as-deposited Cu on $\alpha$-$Al_2O_3$(0001) can be transformed into Cu(111) with centimeter-sized grains. Employing optical microscopy, x-ray diffraction, and electron backscatter diffraction to characterize the films before and after annealing, we find a particular as-deposited grain structure that promotes the growth of giant grains upon annealing. To demonstrate one potential application of such films, we grow graphene by chemical vapor deposition on wafers of annealed Cu and obtain epitaxial graphene grains of 0.2 mm diameter. *This is a work of the U.S. Government and is not subject to copyright protection in the United States.* [http://dx.doi.org/10.1063/1.4817829]

## I. INTRODUCTION

Vapor-phase thin film deposition, first enabled by the invention of modern vacuum technology about a century ago,[1] has developed into an essential component of many modern technologies. Advances in electron diffraction and microscopy over the past century provided tools for probing the crystalline structure of thin films and spurred investigation of the fundamental processes that determine grain size and orientation.[2] Thus grain growth and epitaxy have become central topics in thin film research. In applications of thin films, much effort is spent manipulating grain structure to achieve specific mechanical, electrical, magnetic, optical, and chemical properties. Examples include magnetic recording media,[3] electrochemical catalysts,[4] and interconnects for microelectronics whose resistance to electromigration depends on film texture and grain size.[5] A common challenge for metals and semiconductors grown on insulating substrates is to obtain a desired orientation of grains (such as ⟨111⟩ perpendicular to the film plane) along with macroscopic grain sizes ($\gtrsim$100 $\mu$m in the plane of the film). The conventional approach to this challenge to is to seek conditions that produce large epitaxial grains during growth. An alternative approach, and the one that is the focus of this work, is to deposit a polycrystalline film and then produce large epitaxial grains by annealing. Although the basic idea was clearly described almost 25 years ago by C. V. Thompson *et al.*, who called it "epitaxial grain growth",[6] it has remained relatively unexplored since then. Here we show that this approach can produce films with individual grains with area $>1$ cm$^2$.

The work described here was motivated by a desire to produce Cu(111) films that approach the ideal of a single crystal and that are suitable as substrates for chemical vapor deposition (CVD) of graphene and hexagonal boron nitride (h-BN) at temperatures near 1000 °C. Copper is the most

[a]Official contribution of the National Institute of Standards and Technology; not subject to copyright in the United States.
[b]Electronic address: david.miller@nist.gov
[c]Electronic address: mark.keller@nist.gov

commonly used substrate for graphene CVD because its negligible carbon solubility enables growth of precisely one layer over a wide range of growth conditions. It can also be readily etched away to allow transfer of the graphene to other substrates for further device fabrication steps.[7] Although polycrystalline Cu foils are typically used, the Cu(111) surface provides a hexagonal template with a relatively small lattice mismatch (3.8% and 2.2% for graphene and h-BN, respectively) that allows epitaxial growth with low, uniform strain.[8] Previous work on bulk single crystals has shown that graphene has less rotational disorder when grown on Cu(111) than on Cu(100).[9,10] Exploiting the benefits of Cu(111) for commercial, wafer-scale production of graphene will require a process for producing crystalline films on a suitable substrate. A particularly attractive substrate is $\alpha$-$Al_2O_3$(0001). It is widely used by manufacturers of radio-frequency electronics and light-emitting diodes in the form of wafers with diameters up to 200 mm, it is physically and chemically stable under graphene CVD conditions, and it can likely be reused after metal etching to release the graphene layer.

There is a large body of work pertaining to Cu on $\alpha$-$Al_2O_3$, which is a model system for epitaxy, adhesion, and other properties of metal-ceramic interfaces.[11] On the $\alpha$-$Al_2O_3$(0001) surface, Cu grows epitaxially with a (111) texture, i.e. $(111)_{Cu}\|(0001)_{Al_2O_3}$, and with two distinct in-plane orientation relationships (ORs). The most commonly observed OR (typically referred to as OR I) is $\langle 110\rangle_{Cu}\|\langle 10\bar{1}0\rangle_{Al_2O_3}$. The second OR, called OR II, is $\langle 110\rangle_{Cu}\|\langle 2\bar{1}\bar{1}0\rangle_{Al_2O_3}$. The two ORs differ by a rotation of 30° about $\langle 111\rangle$. Several studies have found that the dominant OR depends sensitively on substrate preparation,[12–14] substrate temperature,[11] deposition rate,[11] and other conditions.[15] We show here that a particular mixture of OR I and OR II in as-deposited Cu films enables giant grain growth upon annealing.

Grain growth in thin films can occur during deposition and during subsequent processing steps such as annealing.[16] The equilibrium state of a film is determined by the interplay of various energies: film-substrate interface, film free surface, grain boundary, and strain. The actual state of a film is also affected by kinetic processes such as diffusion, thus substrate temperature and the energy of arriving species during deposition are important in determining grain size and orientation. Due to the interplay among various energies, conventional grain growth stagnates when the average grain size is about 3 × the film thickness.[16] In some cases, particularly for Cu and other fcc metals where grain boundaries are mobile at relatively low temperatures, grains can grow larger than the stagnation limit through a process known as secondary grain growth.[17] This occurs when grains of a particular low energy orientation grow at the expense of a matrix of other, stagnated grains. Although secondary grain growth can occur during deposition, it is typically exploited during subsequent annealing,[6] as we do here. In Cu films sputtered onto amorphous $SiO_2$, secondary grain growth driven by minimization of strain energy has produced grains ∼10 $\mu$m to ∼100 $\mu$m across with a (100) orientation.[18,19] In our epitaxial Cu films, the fact that a (111) orientation is favored indicates surface and interface energies dominate over strain energies .[16,20]

Annealing can cause a thin film to break into discontinuous islands, a phenomenon known as dewetting or agglomeration.[21,22] The process, which is driven by minimization of the total energy of the film/substrate system, typically begins with the development of thermal grooves at grain boundaries in the film.[23] These grooves deepen at a rate that increases with temperature, and dewetting occurs when the grooves reach the substrate, so thinner films become discontinuous at lower temperatures. For films exposed to temperatures near the bulk melting point, as is the case when Cu (melting point of 1084 °C) is used for CVD of graphene, dewetting is a major limitation on the survivability of the film. Fortunately, grain growth and dewetting are competing processes.[16] As we show here, the growth of giant grains at temperatures somewhat below 1000 °C allows Cu films to endure subsequent graphene growth conditions with minimal dewetting.

In this paper, we present an extensive investigation of grain size and orientation for Cu films sputtered onto $\alpha$-$Al_2O_3$(0001) substrates at a wide range of temperatures, and then annealed at temperatures near 1000 °C. We characterize our films using x-ray diffraction (XRD) and electron backscatter diffraction (EBSD) to measure crystallinity, and optical microscopy to show film properties over large areas. We also report results for large domain graphene growth by CVD on these films, characterized by optical microscopy and Raman spectroscopy. Our findings show that an appropriate combination of deposition and annealing temperatures can produce Cu(111) single crystal

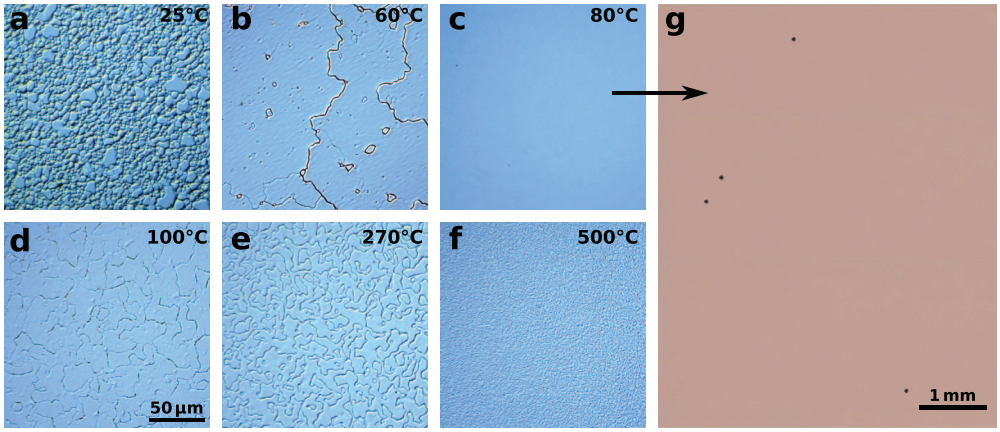


FIG. 1. Giant grains in Cu films after annealing at 950 °C. (a)-(f) Optical images taken using differential interference contrast with a 50 × objective lens. The scale bar in (d) applies to images (a)-(f). Film deposition temperature $T_d$ is indicated in the upper right corner of each image. Dark lines in (b), (d), and (e) are thermal grooves that mark the edges of grain boundaries in the film. The region shown in (c) is a single Cu grain. (g) Conventional optical image of a larger area for $T_d = 80$ °C, stitched from several smaller images, showing the absence of grain boundaries over macroscopic areas. Dark spots are areas of dewetting.

films, free of twinning and thermal grooves, over macroscopic length scales. Such films offer an ideal substrate for epitaxial CVD of graphene, h-BN, and possibly other materials.

## II. RESULTS AND DISCUSSION

### A. Optical microscopy

Figure 1 shows optical microscopy images of Cu films deposited at various temperatures $T_d$ and annealed at temperature $T_a = 950$ °C for 40 min. The annealing conditions were chosen to be similar to those used for graphene CVD, but without the hydrocarbon precursor (see Methods). Images for additional values of $T_d$ and $T_a$ are shown in Supplementary Fig. S1.[24] The dark lines apparent in Fig. 1(b), 1(d), and 1(e) are thermal grooves that mark the edges of grain boundaries in the Cu film (see[25] and Supplementary Fig. S2[24] for confirmation of this correspondence). Since these films are 450 nm thick, conventional grain growth stagnation would limit grains to roughly 3 × the film thickness, or 1.5 $\mu$m. The actual grains are much larger than this limit, and for $T_d = 80$ °C the grains exceed the image size. Figure 1(g) shows a larger area from a $T_d = 80$ °C wafer, and the absence of thermal grooves in this image indicates there are no grain boundaries over the entire area. (See Supplementary Fig. S3[24] for EBSD maps of the rare grain boundaries that remain after annealing.) The dark spots in Fig. 1(g) are areas of dewetting, likely due to microscopic particles introduced during transfer between deposition and annealing steps. Examination of such films with the naked eye shows the Cu grains are typically $\gtrsim$1 cm across. We have observed such giant grain growth on several 50 mm wafers with $T_d = 80$ °C.

### B. X-ray diffraction

It is evident from Fig. 1 that giant grain growth only occurs for a narrow range of $T_d$ near 80 °C. In order to understand the conditions that lead to giant grain growth, we have examined the structure of the Cu films at various $T_d$ using XRD before and after annealing. The XRD results for the as-deposited films, Figs. 2(a)–2(c), reveal a sudden, qualitative change in film properties as $T_d$ increases. For $T_d \leq 80$ °C, we observe: (1) a small (100) component to the film texture (Fig. 2(a), note log scale), (2) broad tails in the rocking curve, which measures misalignment of the ⟨111⟩ vector (Fig. 2(b)), and (3) peaks corresponding to both OR I and OR II in the azimuthal scan (Fig. 2(c)). The peaks every 60° instead of 120° in the azimuthal scans indicate both OR I and

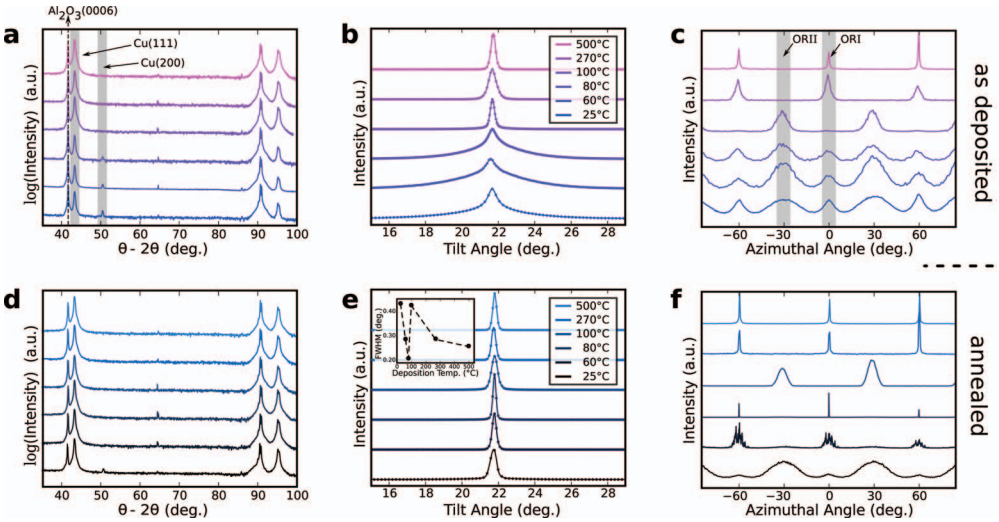


FIG. 2. X-ray diffraction results. (a)-(c) As-deposited films. (d)-(f) Annealed films. Legends in the center panels, (b) and (e), show the deposition temperature $T_d$. The $\theta - 2\theta$ scans in (a) and (d) show the Cu film is predominately (111), with a small (100) component at lower $T_d$ that decreases with annealing. The rocking curves in (b) and (e) show the misalignment of ⟨111⟩ decreases with annealing. The inset of (e) shows the width of the rocking curve after annealing has a sharp minimum at $T_d = 80\,^{\circ}$C. The azimuthal scans in (c) show the complex dependence of as-deposited OR with $T_d$, while those in (f) show the dramatic decrease in orientational disorder for the $T_d = 80\,^{\circ}$C film.

OR II consist of twins that are related by an in-plane rotation of 60°. This twinning, which is expected because the OR between a (111) cubic film and a hexagonal substrate is equivalent for a 60° in-plane rotation, has limited the crystallinity of Cu(111) in several graphene CVD studies.[25–28] For $T_d \geq 100\,^{\circ}$C, the film texture is purely (111), the rocking curve has no tails, and the azimuthal scan shows a single OR. The changes in these three features point to a sudden transition to improved epitaxy between $T_d = 80\,^{\circ}$C and $T_d = 100\,^{\circ}$C. Surprisingly, it is just *below* this transition where giant grain growth is most pronounced, i.e., better as-deposited epitaxy does not necessarily promote giant grain growth upon annealing.

The XRD results for the annealed films, Figs. 2(d)–2(f), show that annealing decreases polycrystallinity for all films: the (100) component is reduced, the rocking curve tails for $T_d \leq 80\,^{\circ}$C are eliminated, and the azimuthal scans show a clear preference for one OR in all cases. The width of the rocking curve peak (inset of Fig. 2(e)) shows a sharp minimum at the value of $T_d$ for which giant grain growth is most pronounced. The azimuthal scan for the $T_d = 80\,^{\circ}$C film shows a complete absence of OR II grains, with sharp peaks at the OR I directions whose width matches the instrumental limit set by beam divergence (see Methods). The azimuthal scan for the $T_d = 60\,^{\circ}$C film shows clusters of sharp peaks, indicating the presence of a few large grains with discrete orientations near the nominal OR I direction.

### C. Electron backscatter diffraction

The XRD results point to a specific polycrystalline state of the as-deposited film that favors giant grain growth. We have used EBSD to study the microstructure of the Cu grains in this polycrystalline state. Texture maps for $T_d = 25\,^{\circ}$C, $80\,^{\circ}$C and $100\,^{\circ}$C are shown in Fig. 3(a)–3(f). The geometry of the EBSD measurement, with definitions of reference, transverse and normal directions (RD, TD, and ND), is shown in Fig. 3(g). Figures 3(a)–3(c) show ND maps, which indicate the out-of-plane direction according to the color scale defined at the right side of the figure, with a (111) pole figure as an inset to each map. Figures 3(d)–3(f) show ND+RD maps where the in-plane component highlights the distinction between OR I and OR II, as shown by the colored squares at the right side of the figure. (For this choice of map, the OR II twins appear as two different colors but both OR I twins appear as a single color.) These maps show a microstucture that is consistent with the

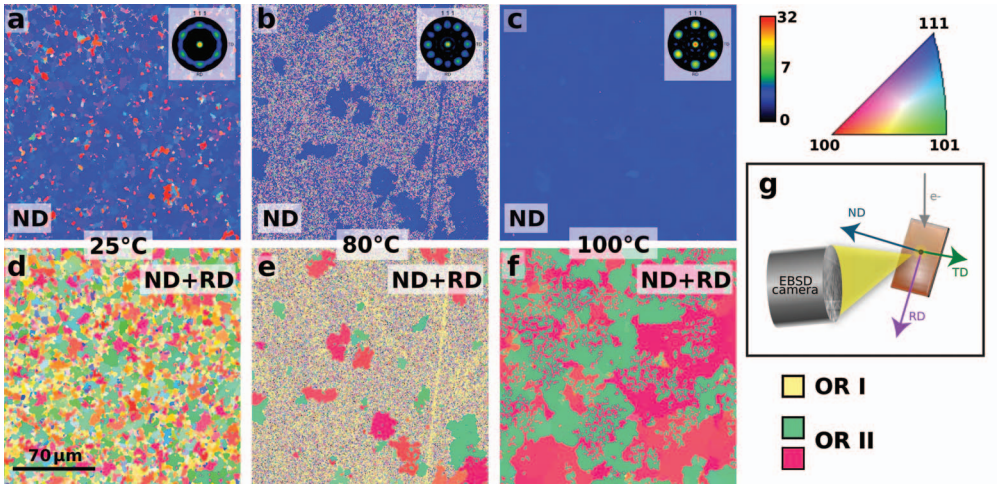


FIG. 3. EBSD texture maps of Cu orientation in as-deposited films. (a)-(c) Maps using the normal direction (ND) for $T_d$ = 25 °C, 80 °C and 100 °C, respectively. The color scale for these maps is shown to the right of the images. Insets show the (111) pole figure for each map, using the logarithmic intensity scale shown at right. (d)-(f) Maps using both normal and and in-plane components (ND+RD). Colors for OR I and OR II are shown to the right of the images. The scale bar in (d) applies to all images in this figure. (g) EBSD geometry showing ND, RD, and TD directions.

XRD results for the corresponding $T_d$ in Figs. 2(a)–2(c). For $T_d = 25\,°C$, the as-deposited film is mostly (111) with a small (100) component that appears as a few red grains in the ND map in Fig. 3(a). The multiple shades of blue in the ND map indicate many grains are somewhat misaligned from (111), which is consistent with the broad XRD rocking curve tails. Both the pole figure and the ND+RD map (Fig. 3(d)) show grains distributed broadly near OR I and OR II in roughly equal proportion. For $T_d = 100\,°C$, only grains close to (111) appear in the ND map (Fig. 3(c)), and the ND+RD map shows only OR II grains (Fig. 3(f)). For $T_d = 80\,°C$, which favors giant grain growth upon annealing, the as-deposited film is marked by a nonuniform distribution of grain sizes: the ND map in Fig. 3(b) shows several (111) grains that are much larger than their neighbors, and the ND+RD map in Fig. 3(e) shows that these large grains are exclusively OR II. The pole figure has 12 spots due to twinning in both the OR II grains (pink and green in Fig. 3(e)) and in the smaller OR I grains (yellow in Fig. 3(e)). The variation of colors for OR II grains is due to in-plane misalignment about the nominal epitaxial direction of up to several degrees. This is consistent with the broad OR II peaks in the XRD azimuthal scans in Fig. 2(c).

Although the large grain size for OR II in Fig. 3(e) indicates OR II is favored over OR I during deposition, the XRD data of Fig. 2(f) show the OR II grains are completely converted into OR I grains during annealing. This suggests the energy difference between OR I and OR II is small and changes sign as temperature is increased. Indeed, previous studies point to the same conclusion: *ab initio*, zero temperature calculations[29] found OR I and OR II differ by 3%, with OR II favored, whereas measurements of the shape of individual Cu particles created by solid-state dewetting at 980 °C indicate a 4% difference with OR I favored.[15] The different in-plane strain expected for the two ORs, tensile for OR I and compressive for OR II,[29] is qualitatively consistent with this finding: since Cu expands more rapidly than $\alpha$-$Al_2O_3(0001)$ as temperature increases, the strain energy of an OR under tensile strain will decrease and that of an OR under compressive strain will increase.

### D. Intermediate stages of grain growth

To examine the intermediate stages of giant grain growth, we used shorter annealing times and lower annealing temperatures. For a $T_d = 80\,°C$ film annealed for ~1 min at 750 °C, we found exclusively OR II grains (Supplementary Fig. S4[24]). After annealing for 20 min at 800 °C, we found individual OR I grains starting to consume the surrounding matrix of OR II grains (Supplementary Fig. S2[24]). Figure 4 shows the boundary between a giant OR I grain

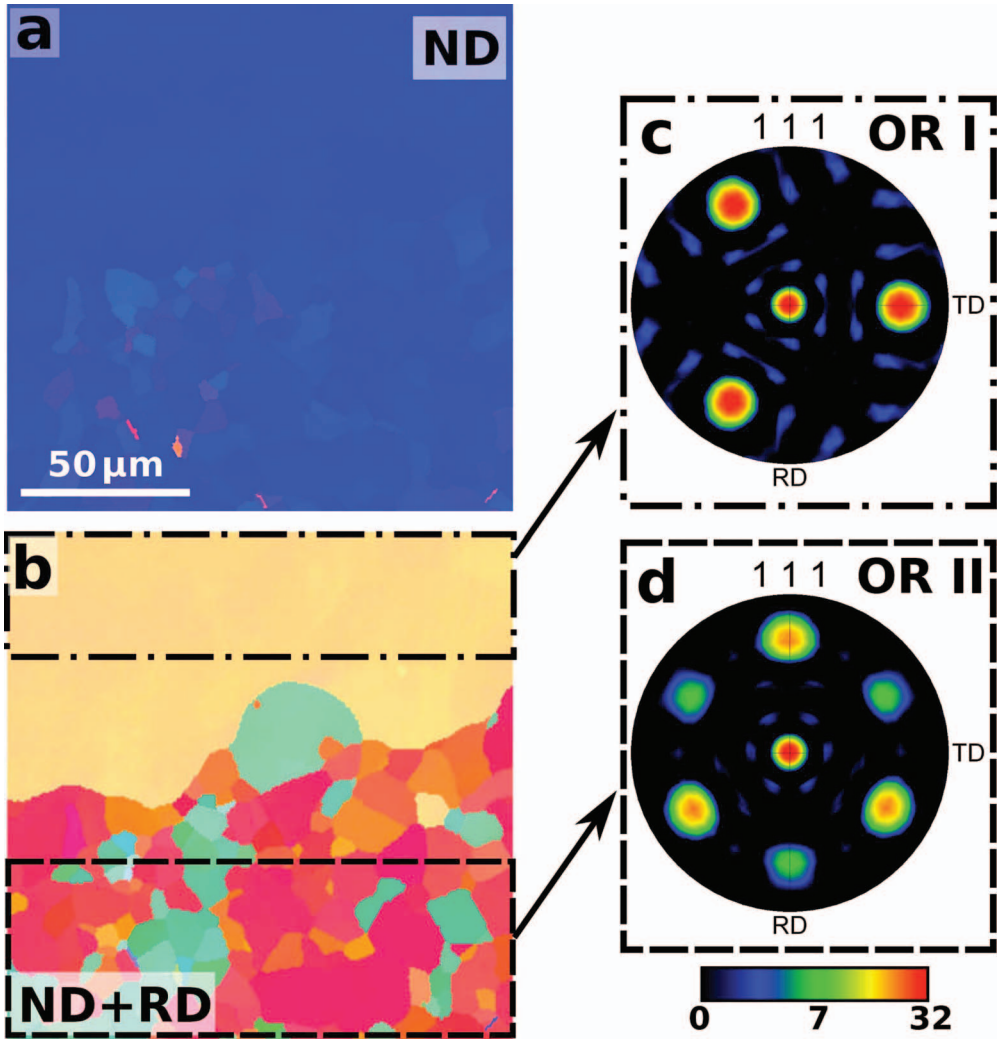


FIG. 4. EBSD maps of boundary between a giant grain and the neighboring matrix. (a) Map using the normal direction (ND). (b) Map of the same region using both normal and and in-plane components (ND+RD). Color scales for both maps are the same as in Fig. 3. (c) Pole figure for the upper region of (b) shows untwinned OR I. (d) Pole figure for the lower region of (b) shows twinned OR II. The logarithmic intensity scale applies to both pole figures.

and the matrix for a $T_d = 80\,^{\circ}C$ film annealed at $T_a = 900\,^{\circ}C$ for 40 min, i.e., as grain growth is nearing completion. Separate pole figures for the upper and lower regions, Figs. 4(c) and 4(d), show that the upper region is a single OR I grain (no twinning) whereas the matrix contains both OR II twins. It is clear that the process of giant grain growth involves OR I grains consuming OR II grains upon annealing. In order for this to occur, the as-deposited film must contain a fraction of both orientation relationships, because if there are no OR I seed grains present (as is the case with $T_d = 100\,^{\circ}C$) or if the film is already exclusively OR I ($T_d \geq 270\,^{\circ}C$), the film will stagnate with the as-deposited orientation relationship, creating thermal grooves between twins and eventually severe dewetting (Supplementary Fig. S1[24]). Deposition at $T_d = 80\,^{\circ}C$ provides a mix of grain orientations that promotes growth of giant OR I grains before significant dewetting occurs, thus stabilizing the Cu film and allowing it to survive graphene CVD conditions. Annealing of a $T_d = 80\,^{\circ}C$ film deposited through a shadow mask to create isolated 100 µm Cu islands showed the density of OR I seed grains is only about one per $mm^2$ (Supplementary Fig. S6[24]).

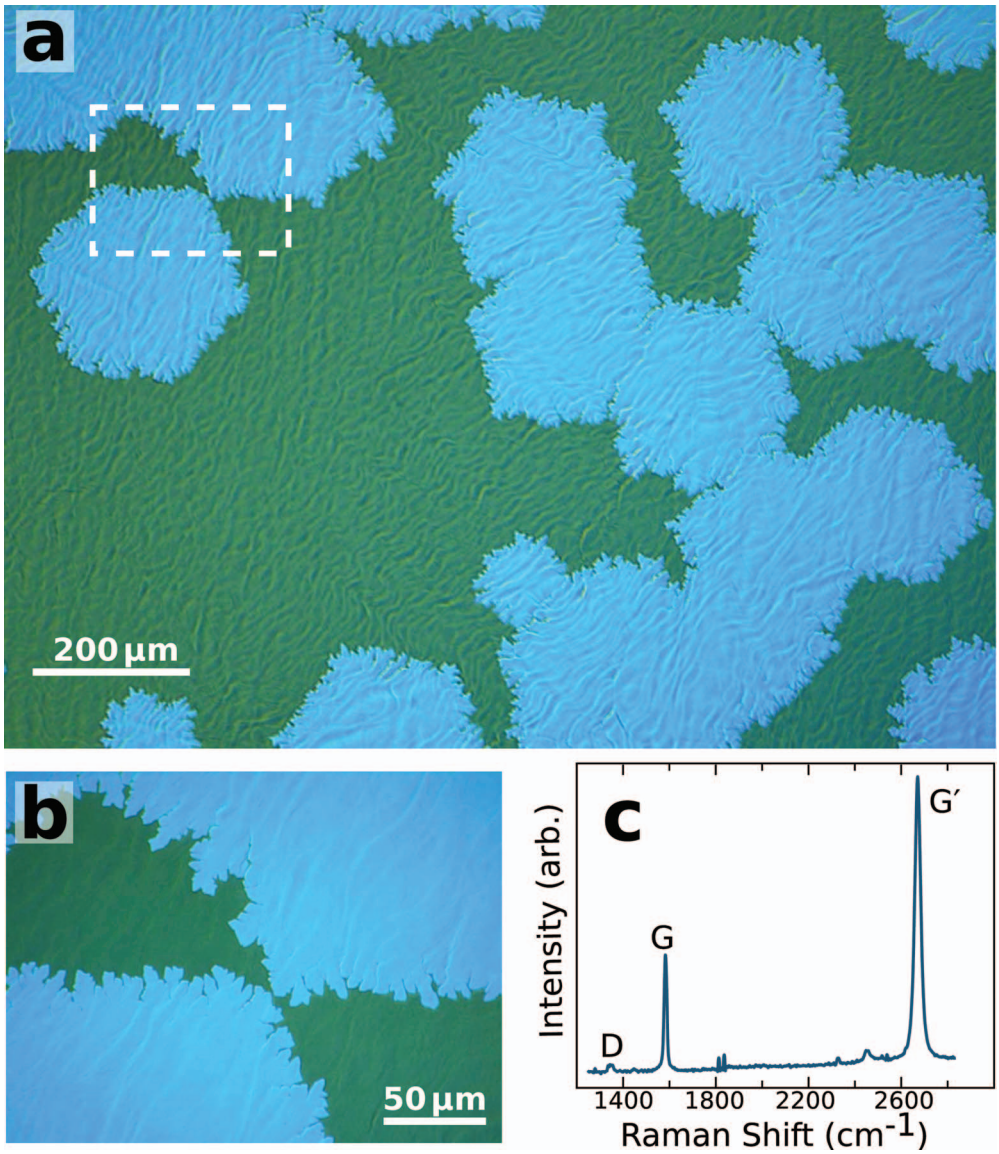


FIG. 5. Graphene growth on giant-grain Cu(111) films. (a) Optical image using differential interference contrast of graphene on Cu after oxidation in air at 180 °C. Oxidized Cu appears darker than the unoxidized regions covered by graphene. (b) Higher magnification image of the region of (a) in the dashed box. (c) Raman spectrum of graphene after transfer to $SiO_2$ substrate.

### E. Graphene growth on giant-grain Cu(111) films

Graphene grown by CVD (see Methods) is shown in Fig. 5. We have optimized the growth parameters for large graphene domains and growth on thin films. Notably, we use an Ar overpressure of 5300 Pa (40 Torr) to suppress Cu sublimation and maintain thin film stability. The image in Fig. 5(a) was taken after stopping growth before a complete graphene layer formed. The sample was baked in air at 180 °C for 5 min to oxidize the bare Cu regions and thus provide optical contrast with unoxidized regions covered by graphene. The graphene islands are roughly 6-fold symmetric, as expected for a Cu(111) surface, and are ≈200 $\mu$m across. Supplementary Fig. S7[24] contains additional images of graphene grown on giant Cu grains. The graphene domains appear to be aligned, suggesting epitaxy and consistent with other results.[28] Since the Cu is epitaxial with the sapphire substrate, this enables alignment of macroscopic features such as sample edges with

zig-zag and armchair directions in graphene nanostructures. Figure 5(b) shows the dendritic nature of the island perimeter. This type of growth is similar to graphene growth at low pressures where the $H_2/CH_4$ ratio is close to 1. Figure 5(c) is a Raman spectrum of the graphene after transfering a continuous graphene film to a 300 nm oxidized Si substrate using PMMA and thermal release tape. The $I_{G'}/I_G$ peak ratio is 2.3, with Lorentzian FWHM peak widths of 12 $cm^{-1}$ and 27 $cm^{-1}$ for the G and G′ peaks, respectively, and the D peak is small. All these features indicate a high quality, monolayer graphene film.

## III. CONCLUSION

We have demonstrated a route to single crystal Cu(111) films over centimeter length scales based on dramatic secondary grain growth of a favored orientation of Cu on $\alpha$-$Al_2O_3$(0001). Our XRD and EBSD results show in detail the particular as-deposited grain structure that promotes giant grain growth upon annealing. Although this work has focused on Cu films thick enough to survive graphene CVD conditions, we expect similar phenomena to occur at lower temperatures for thinner films, based on standard grain growth models. Furthermore, materials other than Cu should also be suitable for giant grain growth if the required as-deposited grain structure can be obtained. A promising candidate is Al on $\alpha$-$Al_2O_3$(0001), since films having a mixture of OR I and OR II have already been demonstrated.[11]

## IV. METHODS

### A. Cu film deposition and annealing

Wafers of crystalline $\alpha$-$Al_2O_3$(0001), 50 mm in diameter, were annealed at 1100 °C in $O_2$ at atmospheric pressure for 24 h to remove scratches due to polishing and give atomically flat terraces. Without further processing, wafers were mounted on a resistively heated Cu puck and placed in a vacuum sputter deposition system. Films of 450 nm nominal thickness were deposited by dc magnetron sputtering from 76 mm targets of 99.999% pure Cu at a rate of ≈1 nm/s. Actual film thickness measured using a profilometer ranged from 430 nm to 500 nm across the wafer, but this variation had no discernable effect on the results. Films with $T_d < 500$ °C were deposited in a load-locked, turbopumped chamber (base pressure $2 * 10^{-7}$ Pa) with a target-to-substrate distance of 8 cm and a sputtering power of 100 $W$ in 0.17 Pa (1.25 mTorr) of Ar. Films deposited at $T_d \geq 500$ °C were deposited in a cryopumped bell-jar-style chamber (base pressure $2 * 10^{-5}$ Pa) with a target-to-substrate distance of 10 cm and a sputtering power of 200 W in 0.67 Pa (5 mTorr) of Ar. The deposition temperature $T_d$ reported here was measured using a thermometer in contact with the sample puck. After deposition, each wafer was coated with PMMA and diced into 5 mm × 6 mm chips. The chips were stripped of PMMA and cleaned by ultrasonic agitation in acetone and isopropanol before characterization and annealing. Annealing was performed in a hot-wall tube furnace with a base pressure of 0.67 Pa (5 mTorr) at temperatures ranging from 950 °C to 1050 °C for a duration of 40 min. The temperature of the furnace was measured using a thermocouple mounted just outside the quartz tube. To suppress Cu sublimation, we maintained a total pressure of 5300 Pa (40 Torr) while flowing 500 sccm 99.999% pure Ar and 11 sccm of 0.2% $H_2$ in Ar, yielding a $H_2$ partial pressure of 0.23 Pa (1.7 mTorr).

### B. XRD and EBSD

X-ray diffraction was performed using a Cu K$\alpha$ source and a 4-circle goniometer with an instrument resolution of 0.0001°. All measurements were performed using parallel beam optics with a maximum beam divergence of 0.15°, which sets the minimum rocking curve linewidth achievable in the experiment. A powder Si sample was used to correct any offsets in the $2\theta$ angle. Symmetric $\theta - 2\theta$ scans were used to determine the out-of-plane crystalline axes. Once the (111) reflection was found, the tilt angle was scanned to generate the (111) rocking curve. In-plane azimuthal scans of the (220) reflection were taken with the grazing incidence angle adjusted to the value of maximum

intensity (typically about 0.5° above the critical angle). At this angle, the entire 5 mm × 6 mm sample is illuminated by the x-rays. Once the (220) peak was located, an azimuthal scan about the sample normal axis was taken to determine the in-plane angular distribution of the [220] axes.

For EBSD measurements, all films were oriented with $[11\bar{2}0]_{Al_2O_3}$ parallel to the RD direction. The SEM accelerating voltage was 20 kV, the chip was tilted 70° towards the detector, and diffraction patterns were collected with 4 × 4 binning over a hexagonal array of ≈500 nm pixels.

### C. Graphene growth, transfer, and characterization

Before graphene growth, the Cu was annealed at $T_a = 950\,^{\circ}C$ for 1 h under 69.5 sccm of 0.2% $H_2$ in Ar to form large grains that are less susceptible to dewetting at higher temperatures. The flow of 0.2% $H_2$ in Ar was then decreased to 11 sccm, giving a $H_2$ partial pressure of 0.23 Pa (1.7 mTorr), and the temperature was ramped to 1055 °C and stabilized for 5 min. Growth was initiated by introducing 14 sccm of 0.2% $CH_4$ in Ar, yielding a $CH_4$ partial pressure of 0.28 Pa (2.1 mTorr). Growth conditions were maintained for 40 min to achieve complete monolayer coverage over an entire chip or wafer. Partial growths were achieved by reducing the growth time. All gases were filtered at the mass flow controller inlets to remove $H_2O$ and $O_2$ contaminants to ∼1 ppb. For transfer of graphene to oxidized Si, PMMA was spun onto the surface and baked at 150 °C, and thermal release tape was applied to the PMMA. Chips were floated on the surface of an ammonium persulfate bath overnight to etch away the Cu. The $Al_2O_3$ substrate fell away, leaving the graphene/PMMA/tape layer on the liquid surface, and this was then rinsed in DI water and placed on a 9 mmx9 mm Si chip with 300 nm of $SiO_2$. The Si chip was heated to 150 °C on a hot plate to release the tape, and then to 180 °C to soften the PMMA and promote adhesion of graphene to the $SiO_2$.[7] To remove the PMMA layer, the chips were submerged in glacial acetic acid for several hours at room temperature. Raman spectroscopy was performed using an excitation wavelength of 532 nm.

## ACKNOWLEDGMENTS

The authors thank Carl Thompson for helpful discussions of grain growth phenomena and Hans Nembach for assistance with Raman spectroscopy. Optical microscope images were taken in NIST's Precision Imaging Facility. Author contributions: D.L.M. and M.W.K. designed the experiments, built custom equipment, and performed film deposition. J.M.S. performed XRD measurements and data analysis. K.P.R., R.R.K., and D.L.M. performed EBSD measurements and analysis. D.L.M. and K.M.D. performed annealing, optical microscopy, graphene growth, and graphene transfer. D.L.M. performed Raman spectroscopy. M.W.K. and D.L.M. wrote the manuscript. All authors discussed the data and commented on the manuscript.

[1] D. Mattox, *The Foundations of Vacuum Coating Technology* (William Andrew Publishing, 2003).
[2] D. W. Pashley, "A historical review of epitaxy," in *Epitaxial Growth, Part A*, J. W. Matthews, Ed. (Academic Press, 1975).
[3] S. N. Piramanayagam, "Perpendicular recording media for hard disk drives," J. Appl. Phys. **102**, 011301 (2007).
[4] D. F. van der Vliet, C. Wang, D. Tripkovic, D. Strmcnik, X. F. Zhang, M. K. Debe, R. T. Atanasoski, N. M. Markovic, and V. R. Stamenkovic, "Mesostructured thin films as electrocatalysts with tunable composition and surface morphology," Nature Materials **11**, 1051–1058 (2012).
[5] C. M. Tan and A. Roy, "Electromigration in ULSI interconnects," Mater. Sci. Engin. Rep. **58**, 1–75 (2007).
[6] C. V. Thompson, J. Floro, and H. I. Smith, "Epitaxial grain growth in thin metal films," J. Appl. Phys. **67**, 4099–4104 (1990).
[7] J. W. Suk, A. Kitt, C. W. Magnuson, Y. Hao, S. Ahmed, J. An, A. K. Swan, B. B. Goldberg, and R. S. Ruoff, "Transfer of CVD-grown monolayer graphene onto arbitrary substrates," ACS Nano **5**, 6916–6924, (2011).
[8] R. He, L. Zhao, N. Petrone, K. S. Kim, M. Roth, J. Hone, P. Kim, A. Pasupathy, and A. Pinczuk, "Large physisorption strain in chemical vapor deposition of graphene on copper substrates," Nano Lett. **12**, 2408–2413 (2012).
[9] S. Nie, J. M. Wofford, N. C. Bartelt, O. D. Dubon, and K. F. McCarty, "Origin of the mosaicity in graphene grown on Cu(111)," Phys. Rev. B **84**, 155425 (2011).
[10] J. M. Wofford, S. Nie, K. F. McCarty, N. C. Bartelt, and O. D. Dubon, "Graphene islands on Cu foils: The interplay between shape, orientation, and defects," Nano Lett. **10**, 4890–4896 (2010).
[11] G. Dehm, H. Edongué, T. Wagner, S. Oh, and E. Arzt, "Obtaining different orientation relationships for Cu films grown on (0001) $\alpha$-$Al_2O_3$ substrates by magnetron sputtering," Inter. J. Mat. Res. **96**, 249–254 (2005).
[12] C. Scheu, M. Gao, S. Oh, G. Dehm, S. Klein, A. Tomsia, and M. Rühle, "Bonding at copper–alumina interfaces established by different surface treatments: a critical review," J. Mater. Sci. **41**, 5161–5168 (2006).

[13] S. H. Oh, C. Scheu, T. Wagner, E. Tchernychova, and M. Rühle, "Epitaxy and bonding of Cu films on oxygen-terminated $\alpha$-$Al_2O_3$(0001) surfaces," Acta Materialia **54**, 2685–2696 (2006).
[14] S. H. Oh, C. Scheu, T. Wagner, and M. Rühle, "Control of bonding and epitaxy at copper/sapphire interface," Appl. Phys. Lett. **91**, 141912 (2007).
[15] S. Curiotto, H. Chien, H. Meltzman, P. Wynblatt, G. S. Rohrer, W. D. Kaplan, and D. Chatain, "Orientation relationships of copper crystals on c-plane sapphire," Acta Materialia **59**(13), 5320–5331 (2011).
[16] C. V. Thompson, "Structural evolution during processing of polycrystalline thin films," Annu. Rev. Mater. Sci. **30**, 159–190 (2000).
[17] C. V. Thompson, "Secondary grain growth in thin films of semiconductors: Theoretical aspects," J. Appl. Phys. **58**, 763–772 (1985).
[18] T. Takewaki, H. Yamada, T. Shibata, T. Ohmi, and T. Nitta, "Formation of giant-grain copper interconnects by a low-energy ion bombardment process for high-speed ULSIs," Mater. Chem. Phys. **41**, 182–191 (1995).
[19] K. Vanstreels, S. Brongersma, Z. Tokei, L. Carbonell, W. De Ceuninck, J. D'Haen, and M. D'Olieslaeger, "Increasing the mean grain size in copper films and features," J. Mater. Res. **23**, 642–662 (2008).
[20] J. Deng, "Phase field modeling of grain growth in thin films on rigid substrates," Phys. Stat. Sol. B **249**, 564–574 (2012).
[21] C. V. Thompson, "Solid-state dewetting of thin films," Annu. Rev. Mater. Res. **42**, 399–434 (2012).
[22] D. Srolovitz and M. Goldiner, "The thermodynamics and kinetics of film agglomeration," JOM **47**, 31–36 (1995).
[23] W. W. Mullins, "Theory of thermal grooving," J. Appl. Phys. **28**, 333–339 (1957).
[24] See supplementary material at http://dx.doi.org/10.1063/1.4817829 for additional figures.
[25] D. L. Miller, M. W. Keller, J. M. Shaw, A. N. Chiaramonti, and R. R. Keller, "Epitaxial (111) films of Cu, Ni, and $Cu_xNi_y$ on $\alpha$ - $Al_2O_3$ (0001) for graphene growth by chemical vapor deposition," J. Appl. Phys. **112**, 064317 (2012).
[26] K. M. Reddy, A. D. Gledhill, C.-H. Chen, J. M. Drexler, and N. P. Padture, "High quality, transferrable graphene grown on single crystal Cu(111) thin films on basal-plane sapphire," Appl. Phys. Lett. **98**, 113117 (2011).
[27] M. Ishihara, Y. Koga, J. Kim, K. Tsugawa, and M. Hasegawa, "Direct evidence of advantage of Cu(111) for graphene synthesis by using Raman mapping and electron backscatter diffraction," Mater. Lett. **65**, 2864–2867 (2011).
[28] B. Hu, H. Ago, Y. Ito, K. Kawahara, M. Tsuji, E. Magome, K. Sumitani, N. Mizuta, K. Ikeda, and S. Mizuno, "Epitaxial growth of large-area single-layer graphene over Cu(111)/sapphire by atmospheric pressure CVD," Carbon **50**, 57–65 (2012).
[29] A. Hashibon, C. Elsässer, and M. Rühle, "Structure at abrupt copper–alumina interfaces: An *ab initio* study," Acta Materialia **53**, 5323–5332 (2005).